

# Shock Waves in Bubbly Liquids

Leen van Wijngaarden

## 1.1 Introduction

The structure of shock waves in bubbly liquids is governed by the behavior of the bubbles. Therefore this chapter starts with a survey of bubble dynamics. This includes the Rayleigh–Plesset equation for bubble oscillations, and the related Minnaert frequency for volume oscillations. A striking property of bubbly liquids is the low sound velocity even at small gas concentration. This is also discussed in Sect. 1.2, together with a survey of linear acoustic waves. Whereas in single phase media a shock wave is formed as a balance between the tendency of a compressive wave to nonlinear steepening on one hand and viscous dissipation on the other, the mechanism opposing steepening is in bubbly liquids dispersion rather than viscous dissipation. This leads as in other areas to the Korteweg–deVries (KdV) equation. Another mechanism of importance is relaxation. These various subjects are treated in Sects. 1.3 and 1.4 before in Sects. 1.4 and 1.5 shock waves are dealt with, strong shocks in Sects. 1.5 and 1.6 and moderately strong in Sect. 1.5/Sect. 1.6.

Since moderately strong waves obey the KdV equation there is an opportunity to put the so-called inverse scattering theory to a test. According to this an expansion wave evolves, as opposed to a compressive wave, in a finite number of solitons. In Sect. 1.6 experiments with an expansion wave are described and comparison with the corresponding theory is made.

## 1.2 Elements of Bubble Dynamics

Central in dealing with shock waves in bubbly flows is the response of a bubble to a pressure perturbation in the surrounding liquid. This is described by the Rayleigh–Plesset equation

$$\rho_l R \ddot{R} + \frac{3}{2} \rho_l \left( \dot{R} \right)^2 = p_g - p_\infty - \frac{4\mu_l}{R} \dot{R}. \quad (1.1)$$

The radius of a bubble, supposed to be spherical, is indicated with  $R$ , the dot on  $R$  indicating time derivative, the liquid density with  $\rho_l$ , the liquid viscosity with  $\mu_l$ , the gas pressure in the bubble with  $p_g$  and the pressure in the incompressible liquid far away from the bubble with  $p_\infty$ . With cavitation bubbles vapor pressure and surface tension are of importance as well. For our subject they have minor importance. If we exclude diffusion of gas from outside into the bubble or vice versa, the mass of gas inside the bubble remains constant

$$R^3 \rho_g = \text{constant}. \quad (1.2)$$

To fully describe the bubble behavior, we need the energy equation both for the surrounding liquid as well as for the gas inside the bubble. Because of the huge difference in heat capacity between liquid and gas we can consider the liquid to be constant in temperature. The energy equation for a perfect gas is

$$\rho_g C_p \frac{D_g T_g}{D_g t} - \frac{D_g p_g}{D_g t} = K \nabla^2 T_g. \quad (1.3)$$

In this equation  $T_g$  is the temperature of the gas in the bubble,  $K$  and  $C_p$  the heat conduction and specific heat, respectively, whereas  $D_g/D_g t$  is the material derivative.

The heat diffusion coefficient for the gas inside a bubble,  $\chi$ , is defined by

$$\chi = \frac{K}{\rho_g C_p}. \quad (1.4)$$

In air  $\chi$  is about  $2 \cdot 10^{-5} \text{ m}^2 \text{ s}^{-1}$ . With a gas temperature variation of angular frequency  $\omega$  the outside temperature penetrates to a depth of order  $(\chi/\omega)^{1/2}$ . This permits in a few limiting cases to avoid the need to use the energy equation as such. To identify such cases we compare  $(\chi/\omega)^{1/2}$  with the bubble radius  $R$  and the wavelength  $l_g$  of the pressure wave in the gas in the bubble. When  $l_g$  exceeds  $R$  and the latter is small with respect to  $(\chi/\omega)^{1/2}$ , we may consider the gas as isothermal. When the first assumption still holds but  $R$  is large with respect to  $(\chi/\omega)^{1/2}$ , the gas content is adiabatic. This remains the case, at increasing frequency, when the wavelength gets smaller than  $R$ . Finally, however, because  $(\chi/\omega)^{1/2}$  shrinks at increasing frequency as  $(\omega)^{-1/2}$  and  $l_g$  as  $(\omega)^{-1}$  pressure changes are isothermal again. A summary is provided in Table 1.1.

An important quantity is the natural frequency for volume oscillations of bubbles, the so-called Minnaert [1] frequency. With a polytropic index  $\kappa$  (in air  $\kappa$  is one for isothermal and 1.4 for adiabatic behavior), this is

$$f_b = \frac{\omega_b}{2\pi} = \frac{1}{2\pi} \left( \frac{3\kappa p_g}{\rho_l R^2} \right)^{1/2}. \quad (1.5)$$

This frequency can be deduced from (1.1) when small excursions from equilibrium are assumed. For air bubbles of a few mm radius  $f_b R \sim 3 \text{ KHz mm}$

**Table 1.1.** Thermodynamic behavior of oscillating gas bubbles

Frequency range	Lengths	Thermodynamic behavior
Low	$1 < \frac{\chi}{\omega R^2} < \frac{l_g}{R}$	Isothermal
Moderately high	$\frac{\chi}{\omega R^2} < 1 < \frac{l_g}{R}$	Adiabatic
High	$\frac{\chi}{\omega R^2} < \frac{l_g}{R} < 1$	Adiabatic
Very high	$\frac{l_g}{R} \ll \frac{\chi}{\omega R^2} \ll 1$	Isothermal

gives a good and quick estimate. For frequencies of this order of magnitude the wavelength  $l_g$  is in air several cm, much larger than the bubble radius. This allows us to consider the pressure inside the bubble as uniform, which as first observed by Nigmatulin and Kabeev [2], permits a simplification of (1.3). With a perfect gas with  $\gamma = C_p/C_v$  we have as constitutive equation

$$\frac{\gamma}{\gamma - 1} p_g = C_p \rho_g T_g. \quad (1.6)$$

The continuity equation for the gas, moving with velocity  $\mathbf{v}$ , inside the bubble is

$$\frac{D_g \rho_g}{D_g t} + \rho_g \nabla \cdot \mathbf{v} = 0. \quad (1.7)$$

Using (1.6) and (1.7) and introducing the radial coordinate  $r$  inside the bubble we obtain from (1.3)

$$r^2 \frac{D_g p_g}{D_g t} - \gamma p_g \frac{\partial v}{\partial r} = (\gamma - 1) \frac{\partial}{\partial r} \left( r^2 \frac{\partial T}{\partial r} \right). \quad (1.8)$$

This is still general. Now we take the pressure uniform inside the bubble,  $D_g p_g / D_g t$  becomes  $\partial p_g / \partial t$ . We can integrate the terms of (1.8) over  $r$  and obtain, with  $(v)_{r=R} = \partial R / \partial t$ ,

$$\frac{\partial p_g}{\partial t} = \frac{3}{R} \left[ (\gamma - 1) K \left( \frac{\partial T}{\partial R} \right)_{r=R} - \gamma p_g \frac{\partial R}{\partial t} \right]. \quad (1.9)$$

The relation (1.9) will turn out to be useful when we come to shock waves.

Now consider a mixture of liquid and bubbles, with concentration by volume  $\alpha$ . At frequencies well below  $\omega_b$  we can neglect the inertia of the fluid pushed away by an expanding bubble or rushing towards where a bubble collapses and take the pressure in the liquid and in the gas to be the same locally. We have a homogeneous fluid with density

$$\rho = \alpha \rho_g + (1 - \alpha) \rho_l. \quad (1.10)$$

If we further assume that there is no relative velocity between bubbles and liquid, we have the condition that the mass of gas in a unit mass of the mixture must remain constant

$$\frac{\alpha \rho_g}{\alpha \rho_g + (1 - \alpha) \rho_l} = \text{constant}. \quad (1.11)$$

With the help of equations of state for gas (1.6) and liquid we can calculate the speed of sound using (1.10) and the expression for the compressibility

$$\frac{1}{c^2} = \frac{d\rho}{dp} = (1 - \alpha) \frac{d\rho_l}{dp} + (\rho_g - \rho_l) \frac{d\alpha}{dp} + \alpha \frac{d\rho_g}{dp}. \quad (1.12)$$

In the case of adiabatic behavior of the gas this gives

$$\frac{1}{c_{\text{ad}}^2} = \frac{d\rho}{dp} = \frac{(1 - \alpha)^2}{c_l^2} + \frac{\alpha^2}{c_g^2} + \frac{\rho_l \alpha (1 - \alpha)}{\gamma p}. \quad (1.13)$$

In Fig. 1.1 are drawn curves of  $c_{\text{ad}}$  as described by (1.13) for different values of the ambient pressure.

A striking property of bubbly suspensions becomes immediately clear, the extremely low velocity of sound, even at a small concentration by volume of  $10^{-2}$  of only  $100 \text{ m s}^{-1}$  at atmospheric conditions. This is small with respect to both the velocity of sound in air and in water. At a concentration of 50% it sinks to only  $20 \text{ m s}^{-1}$ . For use in our discussion of shock waves we shall often simplify (1.13) to

$$c_{\text{ad}}^2 = \frac{\gamma p_g}{\rho_l \alpha (1 - \alpha)} \quad (1.14)$$

which approximates (1.13) very well when  $\alpha$  is not close to either zero or unity. For isothermal behavior we have similarly

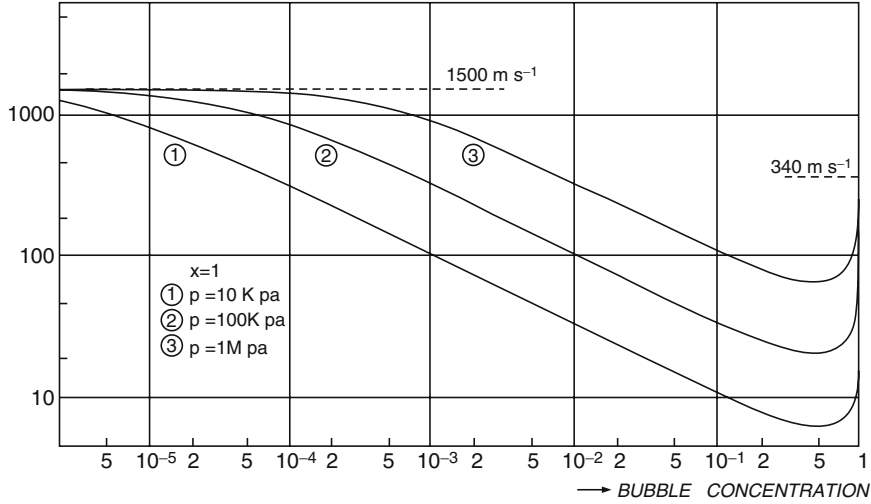


**Fig. 1.1.** Sound velocity as given by (1.13) in bubbly mixture as a function of gas concentration by volume. The three curves are for different ambient pressures

$$(c_{\text{iso}})^2 = \frac{p_g}{\rho_l \alpha (1 - \alpha)}. \quad (1.14a)$$

When the frequency to which bubbles are subjected in the suspension is no longer far below the resonance frequency (1.5) the pressures in liquid and in gas are no longer the same. For small amplitude acoustic waves the presence of the bubbles was accounted for by considering these as point scatterers by Foldy [3] who applied multiple scattering theory to obtain the dispersion equation for linear acoustic waves. van Wijngaarden [4] proposed for waves of arbitrary amplitude the following model:

Similar to (1.7) we can for the bubbly mixture as a whole write the conservation of mass as

$$\frac{D\rho}{Dt} + \rho \nabla \cdot \mathbf{u} = 0, \quad (1.15)$$

and the momentum equation

$$\frac{D\rho \mathbf{u}}{Dt} + \nabla \cdot \rho \mathbf{u} \mathbf{u} + \nabla p = 0. \quad (1.16)$$

Just as  $\rho$  is the local averaged density so is  $\mathbf{u}$  the local averaged velocity and  $p$  the local averaged pressure. In (1.15) and (1.16) the material derivative is

$$\frac{D}{Dt} = \frac{\partial}{\partial t} + \mathbf{u} \cdot \nabla. \quad (1.17)$$

The idea in van Wijngaarden [4] now is to assume the Rayleigh–Plesset equation (1.1) to connect this averaged pressure  $p$  with the local gas pressure in the bubbles giving

$$\rho_l R \frac{D^2 R}{Dt^2} + \frac{3}{2} \rho_l \left( \frac{DR}{Dt} \right)^2 = p_g - p - \frac{4\mu_l}{R} \frac{DR}{Dt}. \quad (1.18)$$

The local volume concentration  $\alpha$  is connected with the local bubble radius  $R$  and the number density of bubbles  $n$  through

$$\alpha = \frac{4}{3} \pi n R^3. \quad (1.19)$$

For the shock waves to be discussed in the following, we shall ignore breaking up of bubbles. Then the number density obeys

$$\frac{\partial n}{\partial t} + \nabla \cdot n \mathbf{v} = 0. \quad (1.20)$$

The equations (1.15)–(1.19), especially (1.18) were formulated by van Wijngaarden [4] without specifying the range of validity. Caffisch et al. [5] have shown that these equations are correct for small  $\alpha$ . They also showed that for a wave entering a quiescent medium, the convective velocities could be neglected.

We consider small amplitude acoustic waves. By linearising (1.1)–(1.3), and (1.16)–(1.20), and assuming a monochromatic wave of the form  $\exp(ikx - \omega t)$  one obtains as dispersion equation

$$\frac{k^2}{\omega^2} = \frac{1}{c^2} \frac{\omega_b^2}{\{(\omega_b^2 - \omega^2) - i\delta\omega\omega_b\}}. \quad (1.21)$$

For details see Prosperetti [6]. For  $\omega \ll \omega_b$ ,  $\omega^2/k^2$  approaches the right hand side of (1.14) or (1.14a) depending on the changes in the bubble being adiabatic or isothermal. For larger values of  $\omega$  (1.21) must be used with for  $c$  and  $\omega_b$  the expressions in (1.14), or (1.14a), and (1.5), respectively. It is interesting to note from (1.5) and (1.14) that both in the adiabatic case and in the isothermal case the quantity  $\omega_b^2/c^2$  is the same, approximately  $4\pi nR$ , and further that for both cases

$$c^2\alpha^2 = \text{constant}. \quad (1.22)$$

The coefficient  $\delta$  in (1.21) represents the wave attenuation. It consists of a part due to viscosity, coming from the last term on the right hand side of (1.18), a part due to thermal conduction, and a part due to acoustic radiation, arising when in the Rayleigh–Plesset equation (1.1) the liquid compressibility is taken into account also, (Prosperetti [6]). For a general time dependent behavior the thermal attenuation cannot be represented by a coefficient as in (1.21). The full energy equation, taking however the simplification (1.9) into account, must be applied. The relation (1.21) says that linear waves are dispersive. The wave equation, ignoring dissipation, is, van Wijngaarden [4],

$$\frac{\partial^2 p}{\partial t^2} - c_0 \frac{\partial^2 p}{\partial x^2} - \frac{R_0^2}{3\alpha_0(1 - \alpha_0)} \frac{\partial^4 p}{\partial t^2 \partial x^2} = 0, \quad (1.23)$$

in which the subscript 0 refers to the equilibrium situation. Equation (1.23) holds for waves in both  $x$  directions. Often we want to look at waves traveling in one direction only, certainly when we have shock waves in mind. An equation valid for waves traveling to the right can be derived in the following way, provided the dispersion is weak. Let us first neglect dispersion. Then the operator in (1.23) can be split up

$$\left( \frac{\partial}{\partial t} - c_0 \frac{\partial}{\partial x} \right) \left( \frac{\partial}{\partial t} + c_0 \frac{\partial}{\partial x} \right) p = 0. \quad (1.24)$$

For a nondispersive wave going to the right  $(\partial/\partial t + c_0\partial/\partial x)p = 0$ . For a right going wave with dispersion this quantity is small, of order  $\varepsilon$ , say, when the dispersion is small. Therefore we may write the first factor in (1.24) as it occurs in the equation with dispersion (1.23) as  $-2c_0\partial/\partial x + O(\varepsilon)$ . Then, correct to  $O(\varepsilon)$ , (1.23) becomes

$$-2c_0 \frac{\partial}{\partial x} \left( \frac{\partial}{\partial t} + c_0 \frac{\partial}{\partial x} \right) p - \frac{R_0^2 c_0^2}{3\alpha_0(1 - \alpha_0)} \frac{\partial^3 p}{\partial x^3} = 0.$$

Integration with respect to  $x$  finally gives

$$\frac{\partial p}{\partial t} + c_0 \frac{\partial p}{\partial x} + \frac{R_0^2 c_0}{6\alpha_0 (1 - \alpha_0)} \frac{\partial^2 p}{\partial x^2} = 0. \quad (1.25)$$

This has the same form as the linearized KdV equation for water waves (see e.g., Whitham [7]), a similarity which will prove to be useful in the following.

### 1.3 Nonlinear Compressive Waves

Since shock waves arise in general from steepening of compressive waves, we start by looking at such a wave. For this purpose we ignore temporarily the effects of bubbles other than their contribution to compressibility. In an  $x, t$  plane a right going characteristic has the direction

$$\frac{dx}{dt} = u + c = c_0 + u + (c - c_0). \quad (1.26)$$

Along the characteristic the sum of the velocity  $u$  and  $\sigma$  is constant where

$$\sigma = \int_{\alpha_0}^{\alpha} \frac{cd\rho}{\rho}. \quad (1.27)$$

In a general motion (1.26) represents a characteristic (see any textbook on gasdynamics e.g., Liepmann and Roshko [8]); the special feature of a simple wave is that all right going characteristics are straight. The wave runs into an undisturbed medium and then  $u = \sigma$ , because along the left characteristics  $u - \sigma = 0$ . It follows from this and (1.26) that in a compressive wave a more compressed part travels faster than a less compressed part and that as a result the wave profile becomes steeper and steeper until at some point the slope is infinite. Making use of (1.10) and (1.14a) it follows that, approximating  $\alpha(1 - \alpha)$  by  $\alpha$ , for the isothermal case

$$\sigma = c_{\text{iso},0} \alpha_0 \ln \frac{\alpha_0}{\alpha} \text{ whereas } c_{\text{iso}} - c_{\text{iso},0} = c_{\text{iso},0} \left( \frac{\alpha_0 - \alpha}{\alpha} \right).$$

Hence a certain value of  $\alpha$  travels in a simple wave with a velocity

$$\frac{dx}{dt} = c_{\text{iso},0} + c_{\text{iso},0} \left( \frac{\alpha_0 - \alpha}{\alpha} + \alpha_0 \ln \frac{\alpha_0}{\alpha} \right). \quad (1.28)$$

For other values of the polytropic index similar relations can be derived. In particular we have for the adiabatic case

$$\frac{dx}{dt} = c_{\text{ad},0} + c_{\text{ad},0} \frac{\alpha_0 - \alpha}{\alpha_0} \left( \frac{\gamma + 1}{2} + \alpha_0 \right). \quad (1.29)$$

Both in (1.28) and in (1.29) the second term in brackets is small in dilute suspensions. This term corresponds to the excess velocity  $u$  in (1.26) and can hence be neglected when the gas concentration is small.

At some point a shock wave forms in a single phase gas. This happens also in a bubbly fluid. However the structure is quite different. The Hugoniot relations are the same. Before the discussion of the structure we give them here. Consider a steady shock traveling with velocity  $U$  into an undisturbed bubbly suspension with pressure  $p_0$  and void fraction  $\alpha_0$ . The corresponding quantities at the other side are  $p_1$  and  $\alpha_1$ . We will restrict to low values of the void fraction and therefore the density may be taken as  $\rho_l(1 - \alpha)$ , see (1.10). Let the shock travel from right to left along the  $x$ -axis. Then in a frame moving with velocity  $U$  to the left the flow is steady. Conservation of mass requires

$$\rho_l(1 - \alpha_0)U = \rho_l(1 - \alpha_1)(U + u_1). \quad (1.30)$$

Next the conservation of momentum must be formulated. Although within the shock all kinds of out-of-equilibrium conditions prevail, equilibrium is reached far upstream and down stream from the shock, resulting in

$$\begin{aligned} p_0 + \rho_l(1 - \alpha_0)U^2 &= p_1 + \rho_l(1 - \alpha_1)(U + u_1)^2, \text{ or using (1.30)} \\ p_1 &= p_0 - \rho_l(1 - \alpha_0)Uu_1. \end{aligned} \quad (1.31)$$

If behind the shock also the temperature is in equilibrium with the surrounding liquid we have from (1.11)

$$\frac{p_0\alpha_0}{1 - \alpha_0} = \frac{p_1\alpha_1}{1 - \alpha_1}. \quad (1.32)$$

In the opposite case in which just behind the shock no heat exchange between bubbles and liquid is supposed to have taken place, this must be replaced by, see (1.11),

$$\frac{p_0^{1/\gamma}\alpha_0}{1 - \alpha_0} = \frac{p_1^{1/\gamma}\alpha_1}{1 - \alpha_1}. \quad (1.33)$$

From (1.30)–(1.33) we obtain the following important expressions for the shock propagation velocity  $U$  for isothermal and adiabatic changes in the gas, respectively,

$$\frac{U^2}{c_{\text{iso},0}^2} = \frac{p_1}{p_0}, \quad (1.34)$$

$$\frac{U^2}{c_{\text{iso},0}^2} = \frac{p_1/p_0 - 1}{1 - (p_0/p_1)^{1/\gamma}}. \quad (1.35)$$

The above Hugoniot relations and the shock speed relation (1.34) were first given by the pioneers Campbell and Pitcher [9] in this subject. They found reasonable agreement with experiments but did not investigate the inner structure of the shocks.



## 1.4 Mechanisms Opposing Steepening of Compressive Waves

### 1.4.1 Viscous Stresses

Apart, of course, from shear stresses viscosity gives the bubbly liquid a bulk viscosity, first noted by Taylor [10] and most easily demonstrated by leaving out in (1.1) the inertia terms

$$p_g - p = \frac{4\mu_1}{R} \dot{R}. \quad (1.36)$$

With help of (1.10), (1.15), and (1.19) and neglecting changes in the number density  $n$  (they are of order  $\alpha$  as follows from 1.20) this can be written as

$$p_g - p = \frac{4\mu_1}{3\alpha} \nabla \cdot \mathbf{u}. \quad (1.37)$$

In gases or fluids in nonequilibrium a difference between the mechanically defined pressure, through the trace of the stress tensor, and the thermodynamic pressure, the one in the constitutive relation, is expressed as the right hand side of (1.37) and the quantity preceding the divergence is called bulk viscosity.

Additional dissipation stems from the relative motion between bubbles and liquid. To see this we introduce the equation of motion of a single bubble in the suspension. Until now we did not need this since we assumed that bubbles move with the liquid. However, when the mixture as a whole is accelerated and the same pressure gradient acts on the continuous phase and on the bubbles, the bubbles acquire a velocity  $\mathbf{v}$  different from the liquid. For one dimensional motion this relative motion is governed by

$$\frac{d}{dt} m (v - u) + f (v - u) = \rho_1 W \frac{Du}{Dt}. \quad (1.38)$$

In this equation  $W$  is the volume of a bubble and  $m$  the added mass, van Wijngaarden [11]

$$m = 1/2 \rho_1 W (1 + 2.78\alpha). \quad (1.39)$$

The first term on the left hand side of (1.38) is the rate of change of the bubble impulse, the second is the viscous friction. For a clean liquid, devoid of surfactants

$$f = 12\pi\mu_1 R. \quad (1.40)$$

The work done by this frictional force adds to the dissipation but this, see van Wijngaarden [12], is not an important effect.

### 1.4.2 Dispersion

We have seen that bubble oscillations make linear waves dispersive, see (1.21) and (1.25). This mechanism may ease the steepening of a compressive wave.

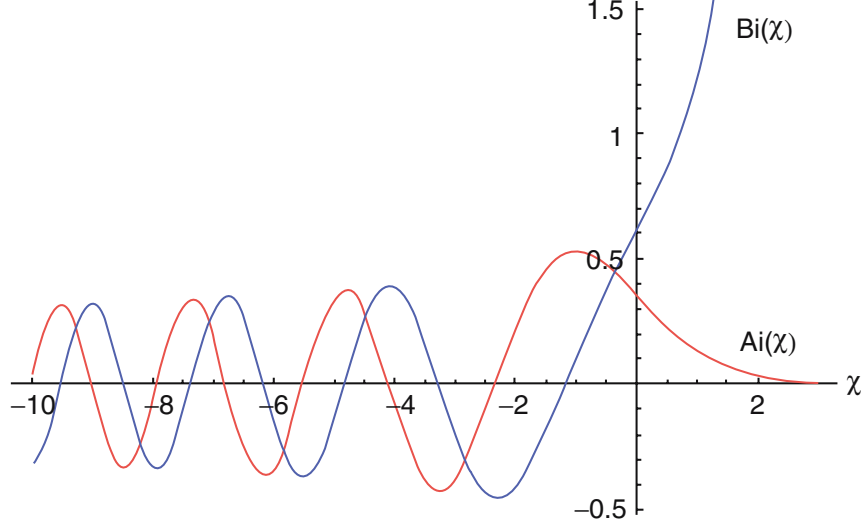


**Fig. 1.2.** How dispersion spreads,  $\text{Ai}(\chi)$ , an original pressure step. The curve  $\text{Ai}(\chi)$  shown is a solution of (1.25)

Consider a linear wave obeying (1.25). Let at time  $t = 0$  the wave profile be a step of strength  $\Delta p/p_0$ . Then (see e.g., Whitham [7], Sect. 13.6) the pressure evolves according to

$$\frac{p - p_0}{p_0} = \frac{\Delta p}{p_0} \int_z^\infty \text{Ai}(s) ds, \quad \text{where } z = \frac{x - c_0 t}{\left\{ \frac{R_0^2 c_0 t}{6\alpha_0(1-\alpha_0)} \right\}^{1/3}}. \quad (1.41)$$

Here  $\text{Ai}$  is the Airy function as drawn in Fig. 1.2, which shows the broadening of the pressure profile.

### 1.4.3 Relaxation

In the theory of shock waves in a single phase gas a well known relaxation process has to do with the nontranslational degrees of freedom of the molecules. These require much more collision times compared with the translational degrees of freedom in order to be in thermal equilibrium with the surroundings. An excellent survey on the implications of this for the propagation of shock waves is given by Lighthill [13]. From these we mention some which are of interest for our purpose. If the rotational and vibrational degrees of freedom do not interact at all with the surroundings, if they are “frozen,” the speed of sound has the highest value, the frozen speed  $c_f$ , say. Each time a

particular degree of freedom starts to take part in the process, a corresponding relaxation time has to elapse for that, the speed of sound decreases. At zero frequency all the internal degrees of freedom are in equilibrium and the speed of sound has the lowest value which we indicate with  $c_e$ . Consider now waves traveling at a speed near, but not quite at,  $c_e$ . It can be shown that the influence of the nonequilibrium degrees of freedom is expressed as a diffusion with effective diffusion coefficient

$$\tau(c_f^2 - c_e^2), \quad (1.42)$$

when there is only one internal degree of freedom with relaxation time  $\tau$ . Of course, these molecular degrees of freedom do not play a role in a bubbly suspension but we can think of the bubbles as molecules. One degree of freedom is the relative velocity of a bubble with respect to the liquid and the other the heat exchange with the surrounding liquid. We shall first, by analogy with the molecular example, inspect what the relative motion, described in Sect. 1.4.1 of this chapter, brings in this connection. Equations (1.38–1.40) show that there exists a relaxation time  $\tau_v$  to accommodate the velocity of a bubble to that of the liquid

$$\tau_v = \frac{R^2}{18\nu_1}. \quad (1.43)$$

With a bubble of radius  $R = 1$  mm and  $\nu_1 = \mu_1/\rho_1 = 10^{-6} \text{ m}^2 \text{ s}^{-1}$ , the value for water,  $\tau_v = 0.06$  s. This means that for motions with a time scale smaller than 0.06 s, or frequencies above about 16 Hz bubbles feel no frictional force and move according to (1.38) but with  $f = 0$ . In this limit the mixture stiffens because a pressure rise is only partly used to compress bubbles. For the rest bubbles are just accelerated out of an elementary volume. The resulting speed of sound is then, van Wijngaarden [12], Noordzij and van Wijngaarden [14] for adiabatic and isothermal motion, respectively,

$$c_{*ad}^2 = \frac{\gamma p (1 + 2\alpha)}{\rho_1 \alpha (1 - \alpha)}, \quad c_{*iso}^2 = \frac{p (1 + 2\alpha)}{\rho_1 \alpha (1 - \alpha)}. \quad (1.44)$$

Comparing these values with those in (1.14) and (1.14a) shows that for both kinds of thermodynamic behavior the sound velocity is higher compared with the case in which bubbles move with the liquid, which corresponds with the equilibrium speed of sound  $c_e$ . The relations in (1.44) are just as those in (1.14) and (1.14a) valid far below the natural bubble frequency. Otherwise they have to be replaced by expressions as in (1.21) in which  $c$  and  $\omega_b$  have the proper value. Noordzij and van Wijngaarden [14] show that, when other effects as heat conduction and dispersion are left out, isothermal pressure waves obey

$$\frac{\partial}{\partial t} \left( c_{*iso}^2 \frac{\partial^2 p}{\partial x^2} - \frac{\partial^2 p}{\partial t^2} \right) + \tau_v^{-1} \left( c_{*iso}^2 \frac{\partial^2 p}{\partial x^2} - \frac{\partial^2 p}{\partial t^2} \right) = 0. \quad (1.45)$$

We now deal with (1.45) in the same way as we did with (1.23) to obtain (1.25). First we choose a wave traveling from left to right at fairly low frequency and take

$$\frac{\partial}{\partial t} + c_{\text{iso}} \frac{\partial}{\partial x} \sim 0.$$

Next we write (1.45) as

$$-c_{\text{iso}} \frac{\partial}{\partial x} \left( c_{* \text{iso}}^2 \frac{\partial^2 p}{\partial x^2} - c_{\text{iso}}^2 \frac{\partial^2 p}{\partial x^2} \right) + 2\tau_v^{-1} c_{\text{iso}} \frac{\partial}{\partial x} \left( c_{\text{iso}} \frac{\partial p}{\partial x} + \frac{\partial p}{\partial t} \right) = 0.$$

Integrating out the derivative with respect to  $x$  finally gives

$$\frac{\partial p}{\partial t} + c_{\text{iso}} \frac{\partial p}{\partial x} - \frac{1}{2} \tau_v (c_{* \text{iso}}^2 - c_{\text{iso}}^2) \frac{\partial^2 p}{\partial x^2} = 0. \quad (1.46)$$

This is exactly as with the molecular relaxation discussed above. We see that the higher order terms, the first two terms on the left hand side of (1.45) act on the wave traveling near the low frequency equilibrium speed as diffusion with coefficient, compare (1.42),

$$\frac{1}{2} \tau_v (c_{* \text{iso}}^2 - c_{\text{iso}}^2). \quad (1.47)$$

In a linear wave a signal eventually dies out by this diffusion but in a nonlinear wave it has, as we shall see, a quite different effect.

Next we discuss heat exchange between bubbles and liquid. Here we have met already the extreme sound velocities, viz.  $c_{\text{ad}}$  and  $c_{\text{iso}}$  as defined in (1.14) and (1.14a). However the relaxation process involved in the increasing accommodation of the bubble temperature to the liquid temperature is not so easy to describe as with the relative motion. This is due to the complicated interplay between the compression and expansion of the bubbles on one hand and the energy budget on the other. The latter is described by (1.3) and the boundary relation (1.9). It is hard for example to define a characteristic relaxation time associated with the heat exchange. If such a time could be found, let us call it  $\tilde{\tau}$ , the diffusion coefficient similar to (1.47) would be

$$\frac{1}{2} \tilde{\tau} (c_{\text{ad}}^2 - c_{\text{iso}}^2). \quad (1.48)$$

## 1.5 Strong Shock Waves

We will now try to describe shock waves in bubbly suspensions, using the concepts and results of previous sections. Pioneers were Campbell and Pitcher [9] who carried out experiments and gave the expression (1.34) for the propagation velocity of the shock waves. They also compared their results with this relation. They carried out the experiments in a vertical shock tube partly filled with an aqueous solution of glycerol in which small air bubbles are suspended. The glycerol is added to keep bubbles small, in their case with radius of the

order of  $10^{-4}$  m. Above this bubbly mixture there is an air filled space closed with a seal. This space is evacuated and subsequently the seal is punctured admitting atmospheric air to enter the tube. The shock wave in air thus created hits the surface of the mixture and now a shock is formed in this mixture. The pressure is recorded at several places along the wall of the tube with help of transducers. All the subsequent investigators used a similar device. In Fig. 1.3 a picture is given of the device used by Noordzij and van Wijngaarden [14].

Campbell and Pitcher [9] experimented with pressure ratios of moderate and large strength. Although the theory regarding processes summarized in Sect. 1.4.3 apply to weak disturbances, the expressions for the speed of the shocks, (1.34) and (1.35) are valid for strong shocks as well. Campbell and Pitcher [9] found good agreement with the isothermal relation (1.34). They did not report data on the shock structure, or the shock thickness. Let us inspect what mechanism would in this case resist the steepening. As a first candidate we consider the bulk viscosity expressed in (1.37). We consider the shock as steady. Just as (1.31) holds for the downstream condition indicated with the subscript 1 it holds for any arbitrary location in the shock

$$p = p_0 - \rho_l(1 - \alpha_0)Uu. \quad (1.49)$$

The corresponding relation for mass conservation, derived from (1.30), is

$$u = \frac{U(\alpha - \alpha_0)}{1 - \alpha}. \quad (1.50)$$

With help of (1.50) and assuming isothermal behavior (the finding of Campbell and Pitcher [9]) we obtain from (1.37) and (1.49), van Wijngaarden [15],

$$(\alpha_0 - \alpha)(\alpha - \alpha_1) = -\frac{4}{3} \frac{\nu_l}{U} \frac{d\alpha}{dx}. \quad (1.51)$$

Strictly speaking we could not apply this to the experiments of Campbell and Pitcher [9] because their shocks are strong but for an order of magnitude analysis it suffices. Solution of (1.51) gives

$$\alpha = \frac{\alpha_0 + \alpha_1}{2} - \frac{\alpha_0 - \alpha_1}{2} \tanh \frac{3U \left(1 - \frac{p_0}{p_1}\right) x}{8\nu_l}. \quad (1.52)$$

This has the same form as the famous Taylor shock, see Lighthill [13], in single phase gases. It follows from (1.52) that the thickness of the shock is of the order of

$$d_v \sim \frac{\nu_l}{U\alpha_0(1 - p_0/p_1)}. \quad (1.53)$$

A typical set of experimental values of Campbell and Pitcher [9] is :  $R = 10^{-4}$  m,  $\nu_l = 1.2 \times 10^{-5} \text{ m}^2 \text{ s}^{-1}$ ,  $U = 41 \text{ m s}^{-1}$ ,  $\alpha_0 = 5 \times 10^{-2}$ ,  $p_0/p_1 = 1/6$ . Introducing this into (1.53) gives for the right hand side about  $10^{-5}$  m, which is smaller than the bubble radius. Just as in a gas the shock thickness

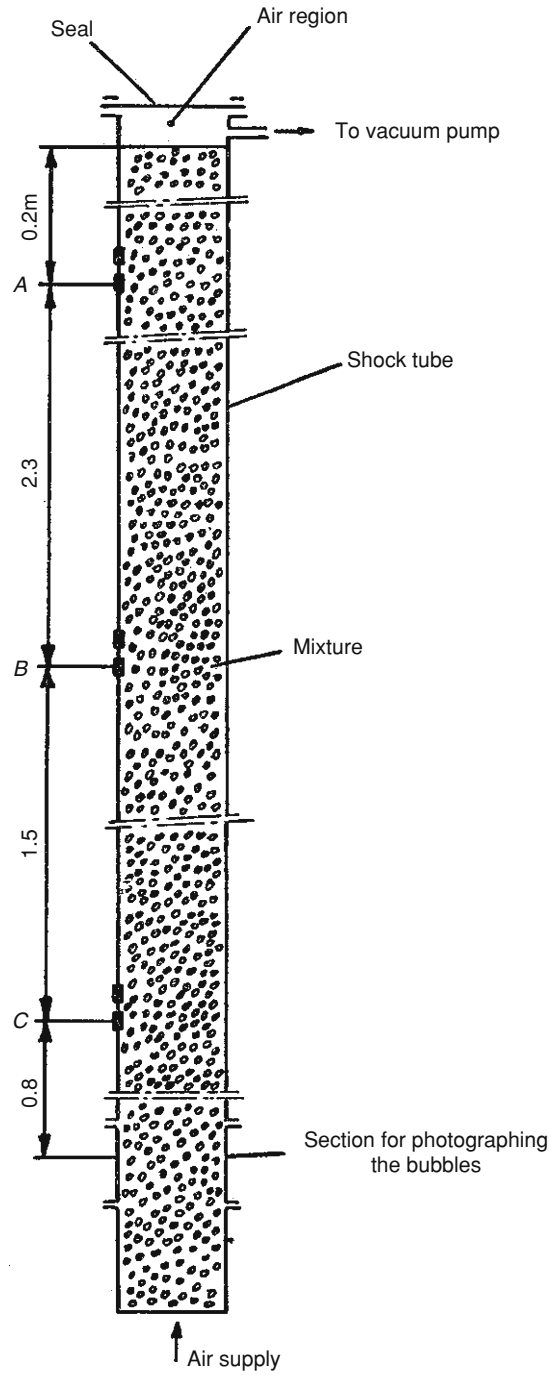


**Fig. 1.3.** Apparatus for measurements on shock waves, from Noordzij and van Wijngaarden [14]. The (*filled square*) indicate the location of pressure transducers

exceeds the mean free path, here the shock should at least cover a few bubble diameters. Since bubbles of radius  $10^{-4}$  m were used this rules out viscosity as the dominant quantity determining the thickness of the shock. We have to look at the mechanisms of dispersion and relaxation. We know how to describe these only for waves of small and moderate strength and hence we will in the following restrict to that type of shocks. Before doing that we make some further remarks on strong shocks. Although no theory exists for strong shocks, except of course the Hugoniot relations, qualitatively they show the same structure as the weaker ones, as shown e.g. in the experiments of Tan and Bankoff [16]. They too used an aqueous solution of glycerol in water and small bubbles, containing argon or nitrogen. So, as long as bubbles remain intact and do not get broken up, much what is said in the following on weak shocks, applies qualitatively to strong shocks as well.

## 1.6 Shock Waves of Moderate and Weak Strength

We saw that due to convection and compression a compressive wave steepens, (1.28) and (1.29), and that viscous dissipation alone is not the opposing mechanism. For weak perturbations, in particular for weak shocks we may, see Lighthill [13], add the terms describing these processes in the evolution equations. For example, taking  $\alpha$  small and assuming isothermal behavior, summation of the nonlinear growth following from (1.28) and the effects of dispersion and dissipation displayed in (1.25) and (1.37), respectively, leads to the evolution equation for  $\tilde{p} = (p_g - p_0)/p_0$ , for a wave traveling to the right,

$$\frac{\partial \tilde{p}}{\partial t} + c_{\text{iso},0} \frac{\partial \tilde{p}}{\partial x} + c_{\text{iso},0} \tilde{p} \frac{\partial \tilde{p}}{\partial x} + \frac{R_0^2 c_{\text{iso},0}}{6\alpha_0} \frac{\partial^3 \tilde{p}}{\partial x^3} - \frac{2}{3} \frac{\nu_1}{\alpha_0} \frac{\partial^2 \tilde{p}}{\partial x^2} = 0. \quad (1.54)$$

The first two terms on the left hand side represent propagation with the sound velocity  $c_{\text{iso},0}$  in the undisturbed medium in which the running coordinate is  $x$ . The third term represents nonlinear steepening in isothermal conditions. The two other terms represent dispersion and dissipation (by bulk viscosity) respectively. This is the so-called Burgers–KdV equation, known from gravity wave theory and other fields, see e.g., Whitham [7]. In formulating the Hugoniot relations we considered a shock going to the left. To treat that case we first formulate the counterpart of (1.54) for waves traveling to the left. In the wave operator in (1.24) we choose now, in  $x^*$ ,  $t$  coordinates  $\frac{\partial}{\partial t} - c_{\text{iso},0} \frac{\partial}{\partial x^*} \sim 0$ , giving instead of (1.54)

$$\frac{\partial \tilde{p}}{\partial t} - c_{\text{iso},0} \frac{\partial \tilde{p}}{\partial x^*} - c_{\text{iso},0} \tilde{p} \frac{\partial \tilde{p}}{\partial x^*} - \frac{R_0^2 c_{\text{iso},0}}{6\alpha_0} \frac{\partial^3 \tilde{p}}{\partial x^{*3}} - \frac{2}{3} \frac{\nu_1}{\alpha_0} \frac{\partial^2 \tilde{p}}{\partial x^{*2}} = 0.$$

Next we look for steady solutions moving to the left with velocity  $U$ . Introducing  $\tilde{p} = \tilde{p}(x^* + Ut) = \tilde{p}(x)$  whence  $\partial/\partial t = U d/dx$  and integrating with respect to  $x$ , we obtain

$$(c_{\text{iso},0} - U)\tilde{p} + \frac{1}{2}c_{\text{iso},0}\tilde{p}^2 + \frac{1}{6}\frac{R_0^2 c_{\text{iso},0}}{\alpha_0}\frac{d^2\tilde{p}}{dx^2} + \frac{2}{3}\frac{\nu_1}{\alpha_0}\frac{d\tilde{p}}{dx} = 0. \quad (1.55)$$

We now use the assumption that the shock is weak to write

$$c_{\text{iso},0} - U = -\frac{1}{2}c_{\text{iso},0}\left(\frac{U^2 - c_{\text{iso},0}^2}{c_{\text{iso},0}^2}\right) = -\frac{1}{2}c_{\text{iso},0}\tilde{p}_1, \quad (1.56)$$

where (1.34) has been used. Introducing this into (1.55) gives

$$\tilde{p}(\tilde{p} - \tilde{p}_1) + \frac{1}{3}\frac{R_0^2}{\alpha_0}\frac{d^2\tilde{p}}{dx^2} + \frac{4}{3}\frac{\nu_1}{U\alpha_0}\frac{d\tilde{p}}{dx} = 0. \quad (1.57)$$

In the last term  $U$  appears instead of  $c_{\text{iso},0}$ , which is correct in the applied approximation, in order to preserve the similarity with (1.51).

It is instructive to derive this equation also from the Hugoniot relations in combination with the extended Rayleigh–Plesset equation (1.18). We start by writing the conservation of momentum (1.49) with help of (1.50) as

$$p + \rho_1 U^2 (\alpha - \alpha_0) = p_0. \quad (1.58)$$

Next we relate the pressure with the gas pressure through (1.18). In Sect. 1.5 we only took the viscous term into account which led to (1.51). Now we take also the first inertia term neglecting the second order term, with  $(DR/Dt)^2$ . Hence, from (1.55) and (1.18), writing  $UdR/dx$  for  $DR/Dt$ , we have

$$p_0 = p_g - \rho_1 R_0 U^2 \frac{d^2 R}{dx^2} - \frac{4\mu_1 U}{R_0} \frac{dR}{dx} + \rho_l U^2 (\alpha - \alpha_0). \quad (1.59)$$

From (1.19) it follows that in the present approximation  $\frac{dR}{dx} = \frac{R_0}{3\alpha_0} \frac{d\alpha}{dx}$ . For isothermal behavior  $\tilde{p}$  can be expressed in terms of  $\alpha$  by

$$\tilde{p} = (p_g - p_0)/p_0 = \frac{\alpha - \alpha_0}{\alpha}. \quad (1.60)$$

Further we have, from (1.34),  $U^2 = p_0/\rho_l \alpha_1$ . Using these expressions (1.59) leads to

$$(\alpha - \alpha_0)(\alpha - \alpha_1) - \frac{R_0^2}{3}\frac{d^2\alpha}{dx^2} - \frac{\nu_1}{3U}\frac{d\alpha}{dx} = 0. \quad (1.61)$$

This equation can with help of (1.60) be cast in terms of  $\tilde{p}$ , resulting again in (1.57).

If adiabatic conditions prevail, the equations are slightly different. We recall that in the absence of dissipation and dispersion a finite disturbance travels with the excess velocity  $(c - c_0) + \sigma$ , see Sect. 1.3. With adiabatic behavior

$$c - c_{\text{ad},0} = c_{\text{ad},0}\tilde{p}\frac{\gamma+1}{2\gamma}, \text{ and } \sigma = \alpha_0 c_{\text{ad},0}\tilde{p}.$$



Just as in the isothermal case the contribution by  $\sigma$  can be neglected for small  $\alpha$ . Then the counterpart of (1.54) reads

$$\frac{\partial \tilde{p}}{\partial t} + c_{\text{ad},0} \frac{\partial \tilde{p}}{\partial x} + \frac{\gamma+1}{2\gamma} c_{\text{ad},0} \tilde{p} \frac{\partial \tilde{p}}{\partial x} + \frac{R_0^2 c_{\text{ad},0}}{6\alpha_0} \frac{\partial^3 \tilde{p}}{\partial x^3} - \frac{2}{3} \frac{\nu_1}{\alpha_0} \frac{\partial^2 \tilde{p}}{\partial x^2} = 0. \quad (1.62)$$

Instead of (1.56) we have in the adiabatic case, using (1.35)

$$c_{\text{ad},0} - U = -c_{\text{ad},0} \tilde{p}_1 \frac{1+\gamma}{4\gamma}. \quad (1.63)$$

Using (1.63) we find in the same way that led from (1.54) to (1.57), from (1.62)

$$\frac{\gamma+1}{2\gamma} \tilde{p} (\tilde{p} - \tilde{p}_1) + \frac{R_0^2}{3\alpha_0} \frac{d^2 \tilde{p}}{dx^2} + \frac{4}{3} \frac{\nu_1}{U \alpha_0} \frac{d\tilde{p}}{dx} = 0. \quad (1.64)$$

The nonlinear equations (1.57) and (1.64) cannot be solved analytically but a lot can be learned by investigating the front and the back. On the low pressure side  $\tilde{p}$  is close to zero and we may replace the quantity in brackets in (1.57) by  $-\tilde{p}_1$  reducing (1.57) to the linear equation

$$\frac{R_0^2}{3\alpha_0} \frac{d^2 \tilde{p}}{dx^2} + \frac{4\nu_1}{3\alpha_0 U} \frac{d\tilde{p}}{dx} - \tilde{p} \tilde{p}_1 = 0. \quad (1.65)$$

The solution that vanishes for  $x \rightarrow -\infty$  is

$$\tilde{p} \sim \exp \left[ -\frac{2\nu_1}{U R_0^2} x + \left\{ \left( \frac{2\nu_1}{U R_0^2} \right)^2 + \frac{3\alpha_0 (p_1 - p_0)}{p_0 R_0^2} \right\}^{1/2} x \right]. \quad (1.66)$$

It follows from (1.65) that with  $R_0 = 0$  we regain the front of the tanh in (1.52). In typical experiments the quantity  $\left\{ \frac{3\alpha_0 (p_1 - p_0)}{p_0 R_0^2} \right\}^{1/2}$  is however dominant. In an experiment of Noordzij and van Wijngaarden [14], to be discussed later in this section,  $R_0 = 1.32 \text{ mm}$ ,  $\alpha_0 = 3.28\%$ ,  $(p_1 - p_0)/p_0 = 0.09$  and  $\nu_1 = 7.10^{-6} \text{ m}^2 \text{ s}^{-1}$ . With these data

$$2\nu_1/U R_0^2 = 0.13 \quad \text{and} \quad \left\{ \frac{3\alpha_0 (p_1 - p_0)}{p_0 R_0^2} \right\}^{1/2} = 71.3.$$

For this kind of bubbles the second of these terms is clearly much larger than the first and the slope at the front is determined by dispersion. We shall therefore assume

$$\frac{2\nu_1}{U R_0^2} \ll \left\{ \frac{3\alpha_0 (p_1 - p_0)}{p_0 R_0^2} \right\}^{1/2}. \quad (1.67)$$

The characteristic scale  $d_A$  at the front is then for isothermal conditions

$$(d_A)_{\text{iso}} = R_0 \left( \frac{p_0}{3\alpha_0 (p_1 - p_0)} \right)^{1/2}. \quad (1.68)$$

Likewise for adiabatic waves, from (1.64)

$$d_{A,ad} = R_0 \left\{ \frac{\gamma + 1}{6\gamma\alpha_0} \frac{p_0}{p_1 - p_0} \right\}^{1/2}. \quad (1.69)$$

Next we inspect the back side of the shock where  $\tilde{p}$  is close to  $\tilde{p}_1$ . Now taking the adiabatic case, we obtain from linearization of (1.64) around  $\tilde{p}_1$ ,

$$\frac{R_0^2}{3\alpha_0} \frac{d^2(\tilde{p}_1 - \tilde{p})}{dx^2} + \frac{4\nu_1}{3U\alpha_0} \frac{d(\tilde{p}_1 - \tilde{p})}{dx} + \frac{2\gamma}{\gamma + 1} \tilde{p}_1 (\tilde{p}_1 - \tilde{p}) = 0. \quad (1.70)$$

The solution which vanishes at  $x \rightarrow \infty$  is

$$\tilde{p}_1 - \tilde{p} \sim \exp \left[ -\frac{2\nu_1}{UR_0^2} x + \left\{ \left( \frac{2\nu_1}{UR_0^2} \right)^2 - \frac{6\gamma}{\gamma + 1} \frac{(p_1 - p_0)\alpha_0}{p_0 R_0^2} \right\}^{1/2} x \right]. \quad (1.71)$$

This predicts that under circumstances for which (1.67) holds, the pressure has the form of damped waves with wavelength  $\lambda$ , see (1.69)

$$\lambda = 2\pi d_{A,ad} = 2\pi R_0 \left\{ \frac{\gamma + 1}{6\gamma\alpha_0} \frac{p_0}{p_1 - p_0} \right\}^{1/2}. \quad (1.72)$$

Similarly, from (1.68) for isothermal conditions

$$\lambda = 2\pi d_{A,iso} = 2\pi R_0 \left( \frac{p_0}{3\alpha_0(p_1 - p_0)} \right)^{1/2}. \quad (1.73)$$

These relations show that the thickness of the shock wave is related to bubble radius rather than molecular mean free path as in single phase gases. For a continuum theory to be valid the thickness should cover at least a few bubble diameters for a single experiment. As (1.69) and (1.72) show this is certainly true for small  $\alpha$  and weak shocks.

How do these predictions compare with experiments? After the pioneering experiments by Campbell and Pitcher [9] who did not investigate the shock structure, experiments of the shock tube type were made by Noordzij and van Wijngaarden [14], Nakoryakov et al. [17], Beylich and Gülhan [18], Tan and Bankoff [16], Kameda and Matsumoto [19]. These experiments show that in the first meter or so after the shock has been formed the structure agrees with the above analysis: a steep rise at the front and waves at the back side. A typical example is in Fig. 1.4, from Noordzij and van Wijngaarden [14], who called this a type *A* shock, a nomenclature adopted later also by Watanabe and Prosperetti [20].

So, qualitatively, this *A* type corresponds with theory. Quantitatively is a different matter as far as the early, [14, 17], experiments are concerned. Let us consider first the thickness and wavelength. When there is agreement it is agreement with the adiabatic rather than the isothermal relation. This can

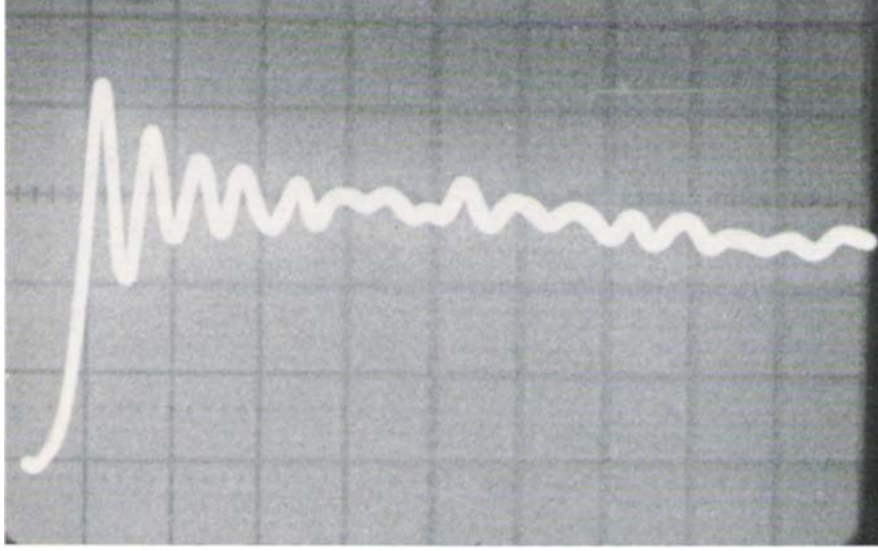


**Fig. 1.4.** An example of an  $A$  shock. Shown is the recording of the pressure in the bubbly suspension.  $R_0 = 1.32$  mm,  $\alpha_0 = 3.28\%$ . From Noordzij and van Wijngaarden [14]

be understood; according to (1.69) and (1.14) the time needed for the shock to pass from the lower to the higher pressure side  $d_{A,ad}/c_{ad}$  is of the order  $R_0(\frac{\rho_l}{p_1 - p_0})^{1/2}$ . The corresponding temperature penetration inside the bubble is

$$\left( R_0 \chi \left( \frac{\rho_l}{p_1 - p_0} \right)^{1/2} \right)^{1/2}. \quad (1.74)$$

With  $R_0 = 10^{-3}$  m,  $\chi = 10^{-5}$  m<sup>2</sup> s<sup>-1</sup> this is only a small fraction of  $R_0$ . While many of the results in [9, 14], agree well with (1.35) and (1.72), others do not. The reason is as pointed out by Nigmatulin [21], that a steady solution of (1.62) has not been reached at a small distance from the entrance in the mixture. Watanabe and Prosperetti [20] set out to compare in a precise way the experimental results with a numerical simulation using the equations proposed by Caffisch et al. [5], which are equivalent with the equations (1.15)–(1.20) given here. Because they were aware of the possible deviations displayed in shocks measured close to the entrance, they compared their results specifically with those obtained by Beylich and Gülhan [18], whose measurements were further from the entrance. They found qualitative agreement, but considerable disagreement in details of the waves at the back of the shock. Figure 1.5 is taken from Watanabe and Prosperetti [20]. It shows experimental results of [18] for an  $A$  shock together with results from their, [20], numerical simulation. (The dotted line will be discussed later).

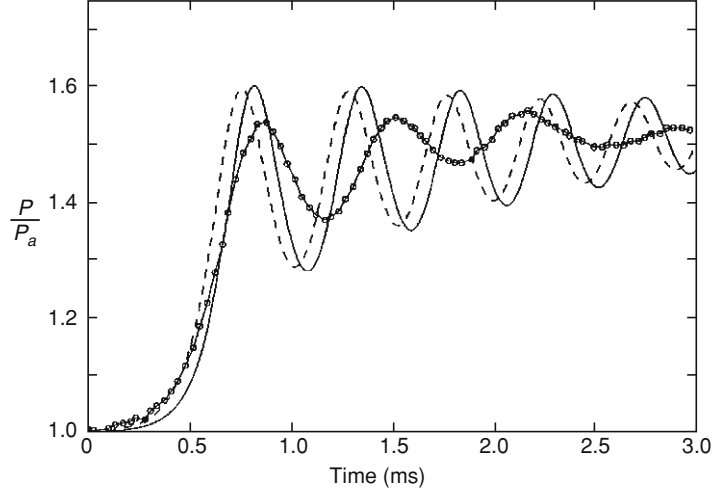


**Fig. 1.5.** Pressure recording in *A* shock. Line with circles shows experimental results of Beylich and Gülhan [18]. *Solid line* shows numerical simulation of Watanabe and Prosperetti [20], whereas the *dotted line* includes relative motion in these simulations

As we will see, other results of the numerical simulation agreed quite well with experimental observations, so it remained a mystery for a while what the reason of the discrepancy as displayed in Fig. 1.5 is. This mystery was solved by Kameda and Matsumoto [19, 22]. While doing experiments they realized that whereas the theories discussed above assume an homogeneous suspension of bubbles, this is not always the case in experiments. In particular the influence of walls renders in vertical devices the transverse distribution inhomogeneous. So, they did two-dimensional numerical calculations for bubble distributions, random in vertical and parabolic in transverse direction. A result is shown in Fig. 1.6a. There is now good agreement with the experimental results. In addition Kameda and Matsumoto [21] did experiments in which care was taken that the bubble distribution was fairly homogeneous. With that precaution they obtained good agreement with the results, for the wave form and wave shape, of experiments. An example is shown in Fig. 1.6b.

Whereas the type *A* shocks are steady solutions of the Burgers–KdV equation (1.62), in all mentioned experiments they were only observed close to the entrance of the shock tube. Deep down they evolve into other forms. This transition is caused by relaxation, discussed in Sect. 1.4. In the beginning steepening is resisted by dispersion as we have seen (as opposed to molecular diffusion in single phase gases). As time proceeds relaxation starts to play an active role. It is, with diffusion coefficients as in (1.47) and (1.48), not able to resist the strong steepening as in the front of an *A* shock. However it may do so at the back of a shock where the slope is much smaller. What we get to observe then is a shock of the type *B*, in the nomenclature of Noordzij and van Wijngaarden [14] and Watanabe and Prosperetti [20].

Shock Wave Science and Technology Reference Library,

Vol. 1

Multiphase Flows I

van Dongen, R. (Ed.)

2007, XVI, 365 p., Hardcover

ISBN: 978-3-540-35845-9